

Excited states in ^{140}Sm above the $(\pi h_{11/2})^2$ and $(\nu h_{11/2})^{-2} 10^+$ isomers

S. Lunardi, D. Bazzacco, G. Nardelli, F. Soramel, J. Rico,* and E. Maglione

Dipartimento di Fisica dell'Università di Padova

and Istituto Nazionale di Fisica Nucleare, Sezione di Padova, Padova, Italy

M. De Poli

Istituto Nazionale di Fisica Nucleare, Laboratori Nazionali di Legnaro, Legnaro, Padova, Italy

G. de Angelis

Istituto Nazionale di Fisica Nucleare, Sezione di Napoli, Napoli, Italy

(Received 1 February 1990)

The level scheme of the $N=78$ nucleus ^{140}Sm has been investigated via in-beam gamma-ray spectroscopy using the $^{114}\text{Cd}(^{30}\text{Si}, 4n)$ reaction. States up to $I=22$ and $E_x=8101$ keV have been established. The level structure above the known isomeric 10^+ states is discussed in terms of the coupling between the valence particles or holes and the $N=78$ and $N=80$ cores.

I. INTRODUCTION

In the $N=78$ isotones ^{140}Sm and ^{142}Gd two isomeric 10^+ states, which lie very close in energy (≤ 40 keV), interrupt the regular ground-state sequence at an excitation energy of about 3.2 MeV.¹ Built on top of the two 10^+ excitations two independent level sequences of stretched $E2$ transitions are observed. The two distinct 10^+ states of single-particle nature are due in this nuclear region^{2,3} to the coupling of two aligned proton particles or two aligned neutron holes in the $h_{11/2}$ orbital. Recent g -factor measurements for the ^{140}Sm nucleus assign a $\pi h_{11/2}^2$ configuration for the 10^+ state at 3211 keV and a $\nu h_{11/2}^{-2}$ configuration for the 10^+ state at 3172 keV.⁴ For the ^{142}Gd nucleus a g -factor measurement was only possible for the 10^+ state at 3165 keV and has identified it as the state built on the $h_{11/2}$ two-proton excitation.⁵ These results confirm the previous identification of the two different single-particle configurations which was based on the characteristically different sequences of levels observed above the 10^+ states. In fact the $E2$ cascades feeding the two isomers closely resemble the ground-state bands of the respective core nuclei [the $N=80$ core for the levels above the $(\nu h_{11/2})^{-2} 10^+$ state and the $N=78$, $Z-2$ core for the levels above the $(\pi h_{11/2})^2 10^+$ state].¹ One may therefore, in both nuclei, interpret the known states above 3.2 MeV simply as the addition of the $N=78$ and 80 core excitations to the respective aligned single-particle 10^+ state.

The alignment of valence nucleons to $\Delta I=2$ core yrast excitations has been discussed within the particle plus rotor and other collective models.^{6,7} Systematic studies, in the framework of those models, of the coupling of the collective excitations of the core with the $h_{11/2}$ proton particle or neutron hole suggest for the $N=80$ and 78 cores opposite nuclear deformations,⁸⁻¹⁰ which therefore coexist at the same excitation energy and at moderately high spin in the $N=78$ nuclei ^{140}Sm and ^{142}Gd .

For the ^{140}Sm nucleus this conclusion was based on the knowledge of only five excited states above the 10^+ isomers up to a maximum spin $I=16^+$. In order to study if the description in terms of shape coexistence is still valid at higher spin, we have reinvestigated the ^{140}Sm nucleus using a heavy-ion beam and a more advanced experimental setup.¹¹ We have been able to place in the level scheme above the 10^+ isomers 43 new levels; this allows us to give a more precise description of the excitation mechanism in ^{140}Sm when the two $h_{11/2}$ proton particles and the two $h_{11/2}$ neutron holes are separately aligned to 10^+ .

II. MEASUREMENTS

The $^{114}\text{Cd}(^{30}\text{Si}, 4n\gamma)$ reaction has been chosen in order to produce high spin states in ^{140}Sm . The ^{30}Si beam was provided by the XTU Legnaro Tandem with typical beam intensities of 1–3 particle nA on target. After a short excitation function measurement a beam energy of 130 MeV has been chosen for the subsequent γ - γ coincidence and γ -ray angular distribution measurements. In the γ - γ coincidence experiments two different ^{114}Cd targets were used. A stack of three 0.5 mg/cm² self-supporting foils was used in one case to permit the decay in flight of the recoiling nuclei. In the second case the target consisted of 1 mg/cm² ^{114}Cd evaporated on a 15 mg/cm² gold foil.

An array of four n -type Ge detectors each one surrounded by a BGO anti-Compton shield was used to collect γ - γ coincidence data. Multiplicity and total γ -ray energy information was obtained using 14 hexagonally shaped BaF₂ crystals positioned vertically seven above and seven below the target chamber and covering a solid angle of about 70%. For both experiments approximately 30 million events were stored onto magnetic tape. The tapes were sorted on a MICROVAX II computer to produce, after careful gain equalization of the germanium energy parameters, a symmetrized matrix of E_γ vs E_γ .

The information from the BaF_2 detectors was used to suppress low multiplicity events from beta decay and from the strong target Coulomb excitation. Examples of background subtracted gated spectra generated from the E_γ vs E_γ matrix are shown in Fig. 1.

For the purpose of spin determination a γ -ray angular distribution measurement was performed, at a beam energy of 130 MeV, using two movable BGO-shielded Ge detectors positioned at five different angles spanning the range 90° – 150° and 30° – 90° , respectively. Two other Ge

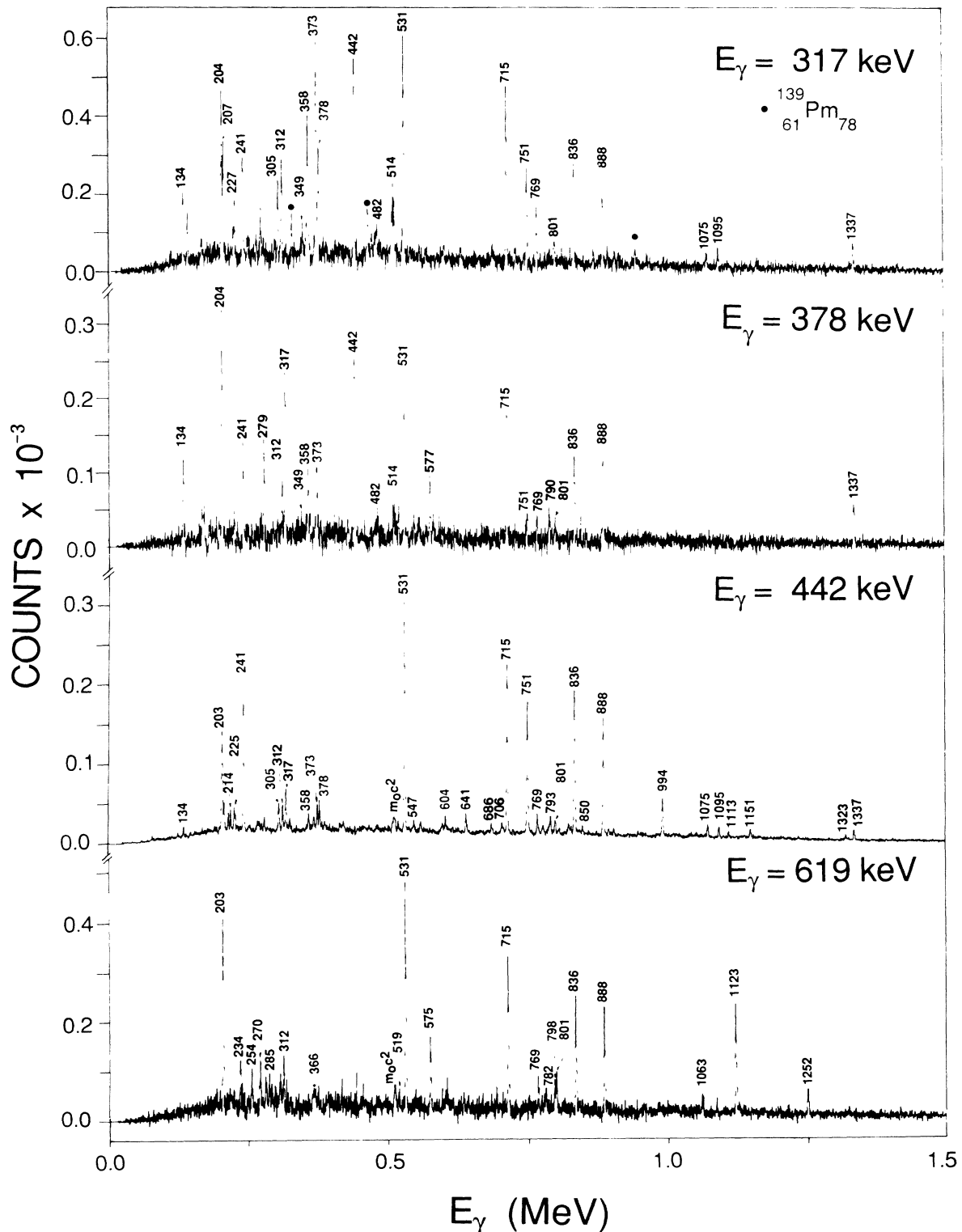


FIG. 1. Background corrected γ - γ coincidence spectra for selected transitions in ^{140}Sm .

TABLE I. Energies, relative intensities and angular distribution data for transitions in ^{140}Sm observed in the $^{114}\text{Cd} + ^{30}\text{Si}$ reaction.

E_γ (keV)	I_γ	A_2/A_0	A_4/A_0	E_x	Assignment
134.3(3)	60(7)			5706	$16 \rightarrow 15^-$
171.3(3)	19(5)	-0.16(13)	-0.13(24)	4854	$13^+ \rightarrow 12^+$
202.6(2)	337(34)	+0.07(10)	-0.05(14)	3172	$10^+ \rightarrow 8^+$
204.2(3)	110(30)			5194	$14^- \rightarrow 13^-$
206.9(3)	24(7)	-0.04(5)	-0.01(6)	5706	$16 \rightarrow 15^-$
218.3(2)	46(10)	-0.37(14)	-0.07(19)	4180	$15 \rightarrow 14^+$
224.9(2)	41(12)	+0.26(10)	+0.14(14)	3194	$8^+ \rightarrow 8^+$
226.9(3)	97(19) ^a	-0.23(9)	-0.24(12)	5706	$16 \rightarrow 15^-$
233.5(3)	66(13)	-0.19(11)	-0.24(15)	5088	$(14^+) \rightarrow 13^+$
241.4(1)	264(26)	+0.23(2)	-0.02(2)	3211	$10^+ \rightarrow 8^+$
254.1(3)	21(5) ^b			6420	
269.7(3)	23(6) ^b			6436	
285.5(3)	43(8)	-0.19(33)	-0.99(47)	5373	$(15^+) \rightarrow (14^+)$
289.6(3)	15(4) ^b			6725	
305.0(3)	45(10) ^b	-0.31(3) ^c	-0.18(5) ^c	5499	$15^- \rightarrow 14^-$
305.0(3)	17(4) ^b			6725	
311.7(1)	189(12)	+0.38(2)	-0.07(3)	2326	$5^- \rightarrow 4^+$
317.4(2)	160(32)	-0.27(2)	-0.14(4)	6024	$17 \rightarrow 16$
324.3(2)	42(7)	-0.55(6)	-0.20(8)	4505	$16 \rightarrow 15$
349.2(3)	9(3) ^b			8101	$(22) \rightarrow (21)$
358.1(2)	53(5)	-0.37(5)	-0.18(7)	6755	$19 \rightarrow 18$
366.1(3)	15(4) ^b	d		7092	
373.5(4)	74(15) ^e	-0.28(9)	-0.06(3)	6397	$18 \rightarrow 17$
377.9(3)	21(9)	-0.31(4)	-0.10(6)	5572	$15^- \rightarrow 14^-$
381.9(3)	38(4)	-0.28(9)	-0.28(14)	4887	$17 \rightarrow 16$
441.9(1)	871(70) ^f	+0.46(1)	-0.05(2)	3653	$12^+ \rightarrow 10^+$
454.2(3)	15(5) ^b	g		7546	
465.5(5)	7(3) ^b	g		5352	$18 \rightarrow 17$
482.4(3)	9(3) ^b			7752	$(21) \rightarrow (20)$
495.6(4)	9(3) ^b			8041	
514.0(3)	19(4) ^b			7269	$(20) \rightarrow 19$
519.5(3)	7(3) ^b			5893	$(16^+) \rightarrow (15^+)$
530.7(1)	1000	+0.26(2)	+0.00(3)	531	$2^+ \rightarrow 0^+$
575.3(2)	64(6)	+0.52(7)	-0.22(9)	5489	$16^+ \rightarrow 14^+$
604.1(2)	41(5) ^b			5998	
618.7(1)	196(20)	+0.45(3)	-0.05(4)	3791	$12^+ \rightarrow 10^+$
632.9(4)	23(7) ^b	g		2959	$\rightarrow 7^-$
640.9(3)	61(6)	-0.29(10)	-0.09(14)	6039	$17 \rightarrow 16^+$
681.7(5)	116(12)	-0.67(11)	+0.08(15)	3092	$11^+ \rightarrow 10^+$
686.2(4)	18(5) ^b				unplaced
715.0(1)	948(50)	+0.22(1)	-0.04(2)	1246	$4^+ \rightarrow 2^+$

detectors, kept at a fixed position, were used as monitors. In order to obtain clean spectra, only events firing one of the germanium detectors and at least three detectors of the multiplicity filter were accepted and written on magnetic tape in list mode for off-line analysis.

The obtained experimental angular distributions were analyzed in terms of the usual Legendre polynomials expansion:

$$W(\theta) = A_0 + A_2 P_2(\cos\theta) + A_4 P_4(\cos\theta),$$

where θ is the angle of the detector measured with respect to the beam axis. The A_2/A_0 and A_4/A_0 coefficients extracted from the fit are listed in Table I. As may be noted the obtained values are somewhat bigger than usual results. This shows that the coincidence with

the BaF_2 detectors, which were positioned in a direction normal to the angular distribution plane, produced a slight alignment of the decaying nuclei.

Additional information on γ -ray multipolarity has been derived from angular correlation results obtained from the $^{114}\text{Cd}(^{29}\text{Si}, 3n)^{140}\text{Sm}$ reaction where the ^{140}Sm nucleus is also populated with considerable cross section. In the γ - γ coincidence experiment with the ^{29}Si beam ($E_{^{29}\text{Si}} = 128$ MeV) six Ge detectors have been used, two positioned at angles close to 90° and the other four positioned as close as possible to the beam line ($\approx \pm 37^\circ$). An angular correlation array has been created with the 90° detectors on one axis and the 37° detectors on the other axis. Gates have been set along both axes on the known $E2$ transitions of the ground-state band, and the intensity

TABLE I. (Continued).

E_γ (keV)	I_γ	A_2/A_0	A_4/A_0	E_x	Assignment
751.3(2)	637(70) ^h	+0.43(2)	-0.09(2)	4404	$14^+ \rightarrow 12^+$
768.8(3)	286(29)	-0.17(3)	-0.00(4)	2014	$5^- \rightarrow 4^+$
771.1(3)	18(5) ^b	d		7320	$(20^+) \rightarrow 18^+$
780.3(4)	21(6)	g		6778	
782.5(2)	51(10)	+0.38(7)	+0.16(10)	6272	$18^+ \rightarrow 16^+$
790.2(4)	20(5) ^b			5194	$14^- \rightarrow 14^+$
790.5(4)	26(8) ^b			4683	$12^+ \rightarrow 11^+$
792.6(4)	44(5) ^b	g		4445	$13^+ \rightarrow 12^+$
801.3(2)	120(12)	+0.29(4)	+0.01(6)	3127	$9^- \rightarrow 7^-$
808.3(3)	13(4) ^b	d		5254	$15^+ \rightarrow 13^+$
825.5(3)	73(7)	+0.35(7)	-0.07(10)	6864	$19 \rightarrow 17$
835.3(5)	110(12) ^b			4488	$14^+ \rightarrow 12^+$
836.1(2)	710(60)	+0.22(1)	-0.03(2)	2082	$6^+ \rightarrow 4^+$
850.5(3)	54(5)	-0.65(9)	-0.01(12)	5254	$15^+ \rightarrow 14^+$
887.6(1)	659(33)	+0.21(2)	-0.06(3)	2969	$8^+ \rightarrow 6^+$
896.3(4)	13(5)	+0.54(7)	-0.47(10)	4024	$11^- \rightarrow 9^-$
906.0(5)	77(8)	+0.03(5)	-0.27(7)	5394	$(16^+) \rightarrow 14^+$
916.4(3)	33(6)	+0.36(15)	-0.02(22)	4044	$11^- \rightarrow 9^-$
993.8(3)	110(9)	+0.46(3)	-0.11(4)	5398	$16^+ \rightarrow 14^+$
1063.4(3)	53(5)	-0.38(8)	+0.09(12)	4854	$13^+ \rightarrow 12^+$
1075.0(2)	83(8)	-0.17(6)	-0.15(9)	5479	$15^- \rightarrow 14^+$
1095.1(2)	58(6)	-0.14(7)	+0.10(11)	5499	$15^- \rightarrow 14^+$
1103.0(4)	22(3)				unplaced
1112.8(3)	50(8)	+0.15(9)	-0.10(13)	3194	$8^+ \rightarrow 6^+$
1123.5(3)	180(30) ⁱ	+0.24(6)	-0.17(8)	4914	$14^+ \rightarrow 12^+$
1151.5(3)	70(9)	+0.25(7)	-0.13(10)	6549	$18^+ \rightarrow 16^+$
1223.1(4)	21(4)	d		7772	$(20^+) \rightarrow 18^+$
1252.0(4)	40(4)	+0.22(11)	-0.28(16)	6166	$16^+ \rightarrow 14^+$
1322.8(7)	31(4)	+0.56(13)	-0.10(17)	5811	$16^+ \rightarrow 14^+$
1337.4(2)	92(9)	-0.16(5)	+0.00(8)	4990	$13^- \rightarrow 12^+$
1406.6(4)	7(3)	+0.80(40)	-0.48(56)	5811	$16^+ \rightarrow 14^+$

^aUnresolved from 226.9 keV line in ^{140}Pm . A_2/A_0 and A_4/A_0 given for complex line.

^bTransition intensity taken from γ - γ coincidence data.

^c A_2/A_0 and A_4/A_0 coefficient given for complex line.

^d $I(90^\circ)/I(37^\circ) \geq 1$ from the angular correlation data.

^eUnresolved from 374.1 keV line in ^{140}Pm . A_2/A_0 and A_4/A_0 given for complex line.

^fUnresolved from 441.5 keV line in ^{139}Sm . The contribution of the ^{139}Sm line is estimated to be 40% of the total intensity.

^g $I(90^\circ)/I(37^\circ) \leq 0.8$ from the angular correlation data.

^hUnresolved from 751.2 keV line in ^{139}Pm , which gives $\sim 50\%$ contribution to the complex line.

ⁱUnresolved from 1124.5 keV transition in ^{141}Sm . A_2/A_0 and A_4/A_0 given for complex line.

of other transitions observed in the two spectra has been extracted. If $I(90^\circ)$ and $I(37^\circ)$ represent the intensity of the transitions when gating on the 90° and 37° axis, respectively, the ratios $I(90^\circ)/I(37^\circ)$ which we obtain are typically ≥ 1 for quadrupole transitions and ≤ 0.8 for dipole transitions. Angular distribution results, relative intensities, and energies of the γ -rays associated with the decay of ^{140}Sm are listed in Table I.

The quoted γ -ray intensities have been extracted from direct spectra taken at 120° , correcting when necessary for contributions of unresolved lines coming from other nuclei. For weak lines the relative intensity has been derived from the γ - γ coincidence data.

III. THE LEVEL SCHEME OF ^{140}Sm

The level scheme of ^{140}Sm obtained from our measurements is shown in Fig. 2. The data confirm the results reported in Ref. 1 and extend the knowledge on the high spin states of ^{140}Sm up to $I \approx 22$ and $E_x = 8.1$ MeV. Many new γ -ray cascades have been observed above the known 10^+ isomers at 3172 keV ($T_{1/2} = 22.3$ ns), and at 3211 keV ($T_{1/2} = 6.2$ ns). Moreover a few new levels are identified also below the two 10^+ states. One of these states lies at an excitation energy of 3194 keV, just between the two 10^+ isomers. This level deexcites to the 8^+ state at 2969 keV and to the 6^+ state at 2082 keV

sitions continues the level scheme up to an excitation energy of 8041 keV. Spin and parity assignments, based on the angular distribution data and on decay branching ratios, confirm the previous assignments to the states up to 16^+ . This fact gave us confidence in establishing the spin and in some cases the parity of the newly identified levels too. Some γ lines show angular distributions with a strong negative value of the A_2/A_0 coefficient [or equivalently they show an unusually small $I(90^\circ)/I(37^\circ)$ ratio in the angular correlation data] and we assign $M1+E2$ multipolarity to the γ lines showing this behavior. Accordingly, when the A_2/A_0 coefficient is typical for a $\Delta I=1$ stretched transition an $E1$ assignment which implies a change of parity is also possible. An example of this is the 769 keV transition connecting the known 5^- state to the 4^+ level of the ground band. The A_2/A_0 and A_4/A_0 coefficients of the 769 keV line may be taken therefore as characteristic of a pure $\Delta I=1$ $E1$ transition. The 1337 keV transition deexciting the state at 4990 keV also has such an angular distribution, and the level sequence built on that state suggests a change of the structure of the nucleus. On this basis we assign $I^\pi=13^-$ to the 4990 keV level.

IV. DISCUSSION

As already pointed out in the Introduction, in the ^{140}Sm nucleus the excited states above the proton and neutron $h_{11/2}^2$ isomers have been successfully interpreted up to 16^+ as the core states coupled to the 10^+ single-particle excitations. In the same spirit we can interpret the new 18^+ state at 6549 keV as the 8^+ excitation of the core nucleus ^{138}Nd coupled to the $(\pi h_{11/2})^2$ 10^+ level. The collective sequence based on the 10^+ state of proton character continues then with a 1223 keV transition giving a state with $I^\pi=(20^+)$ at 7772 keV. This state has no counterpart in the core nucleus; instead at lower energy a 20^+ level is expected due to the alignment of two $h_{11/2}$ neutron holes. In the core nucleus ^{138}Nd , the 10^+ state of neutron character lies 3.2 MeV (Ref. 12) above the ground state, and the corresponding state in ^{140}Sm should lie therefore at 6.4 MeV if no residual interaction is acting in the coupling of the two $h_{11/2}$ neutron holes and the two $h_{11/2}$ proton particles.

We observe indeed a level at 7.32 MeV with probable spin 20 which deexcites through a 771 keV γ -ray transition to the 18^+ level causing a discontinuity in the regularly increasing energy of the transitions of the band built on the $(\pi h_{11/2})^2$ 10^+ state. We interpret the level at 7.3 MeV as the 20^+ fully aligned member of the $\pi h_{11/2}^2 \nu h_{11/2}^-$ multiplet, which is pushed up in energy by 0.9 MeV with respect to the unperturbed 6.4 MeV energy. This can be easily understood since the two $h_{11/2}$ protons and the two $h_{11/2}$ neutron holes coupled to 10^+ have opposite quadrupole moments.^{13,14} An analogous situation is also evident in the odd- Z $N=78$ nuclei ^{139}Pm (Ref. 15) and ^{141}Eu , (Ref. 16) where the fully aligned $\frac{31}{2}^-$ multiplet member of the $\pi h_{11/2} \nu h_{11/2}^-$ configuration is pushed up by at least ~ 0.5 MeV with respect to the core $(\nu h_{11/2})^-$ 10^+ state, since one particle and two holes contribute to this three-nucleon configuration. Further-

more, the ^{139}Pm (Ref. 17) and ^{141}Eu (Ref. 18) nuclei show collective $E2$ sequences built on the $\frac{11}{2}^-$ β -decaying isomer which present two discontinuities; the first one due to the alignment of two $h_{11/2}$ protons at spin $\frac{27}{2}^-$, the second one due to the alignment of two $h_{11/2}$ neutron holes at spin $\frac{47}{2}^-$. The spin $\frac{47}{2}^-$ lying 7.5 and 7.0 MeV above the $\frac{11}{2}^-$ isomer in ^{139}Pm and ^{141}Eu , respectively, is just the fully aligned member of the $(\pi h_{11/2}^3 \nu h_{11/2}^-)$ configuration and corresponds most probably to the 20^+ state at 7.3 MeV in ^{140}Sm .

Beside the 20^+ level there is a close correspondence between the level scheme of ^{140}Sm above the $\pi h_{11/2}^2$ state and the level structure of the odd-proton nucleus ^{139}Pm (Refs. 15 and 17) above the $\frac{11}{2}^-$ state. Similarly, as we will discuss later, we observe also a close resemblance between the states built on the $\nu h_{11/2}^-$ state in ^{140}Sm and the excited states of the odd-neutron nucleus ^{141}Sm above the $\frac{11}{2}^-$ level.¹⁹ In both cases it is apparent that the coupling of one or two $h_{11/2}$ valence particles (or holes) to the corresponding core nucleus (^{138}Nd and ^{142}Sm , respectively) gives rise, in the odd-even and even-even nuclei with one or two more (or less) particles, to a level structure very similar to that of the core nucleus itself.

In our experiment we have identified a series of negative parity states with spin from 13^- to 15^- at $E_x \simeq 5.3$ MeV which deexcite to the 12^+ and 14^+ states of the $\pi h_{11/2}^2$ sequence; a similar series of levels is observed in the odd- Z nucleus ^{139}Pm too.^{15,17} The level scheme of that nucleus (and also of ^{141}Eu) is characterized by a strong $E1$ 1298 keV transition feeding the $\frac{15}{2}^-$ state and which gives origin to a sequence of positive parity states connected by $\Delta I=1$ low-energy transitions. In the ^{140}Sm nucleus the $(\pi h_{11/2}^2 \otimes 2_{\text{coll}}^+)12^+$ level at 3653 keV is the counterpart of the $\frac{15}{2}^-$ state of the ^{139}Pm nucleus and also here we observe a strong $\Delta I=1$ transition (1337 keV) depopulating a 13^- state at 4990 keV above which, again, a sequence of low-energy transitions connecting states of negative parity is observed. These $\Delta I=1$ level sequences, which appear consistently in the odd- Z $N=78$ nuclei and in the ^{140}Sm nucleus when two $h_{11/2}$ protons are aligned, most probably involve the $(\nu h_{11/2}^- s_{1/2}^-)5^-$ and $(\nu h_{11/2}^- d_{3/2}^-)7^-$ excitations which occur systematically in the doubly even $N=78$ isotones. Through the coupling of the $(\pi h_{11/2})^2$ 10^+ state to the higher lying negative parity states of the nucleus ^{138}Nd we can also interpret the two states with spin 17 and 19 which deexcitate through the 641 and 825 keV transitions.

Through in-beam experiments the unfavored members ($\frac{17}{2}^-$, $\frac{21}{2}^-$, $\frac{25}{2}^-$) of the decoupled $h_{11/2}$ band in the odd-even $N=78$ ^{137}Pr (Ref. 20) and ^{139}Pm (Ref. 15) nuclei are also weakly populated. Analogously we interpret the positive parity states shown on the far left of Fig. 2 as the unfavored members of the $(\pi h_{11/2}^2 \otimes \text{core})$ band.

Another characteristic feature of the odd- Z nuclei with $N=78$ is the presence of a fairly strongly populated $\Delta I=1$ sequence^{15,16,20} built on a $\frac{27}{2}^-$ state which is interpreted as the $I_{\text{max}}-2$ member of the $(\pi h_{11/2} \nu h_{11/2}^-)$ multiplet. In view of the very good agreement between the level scheme of ^{140}Sm above the 10^+ of proton character

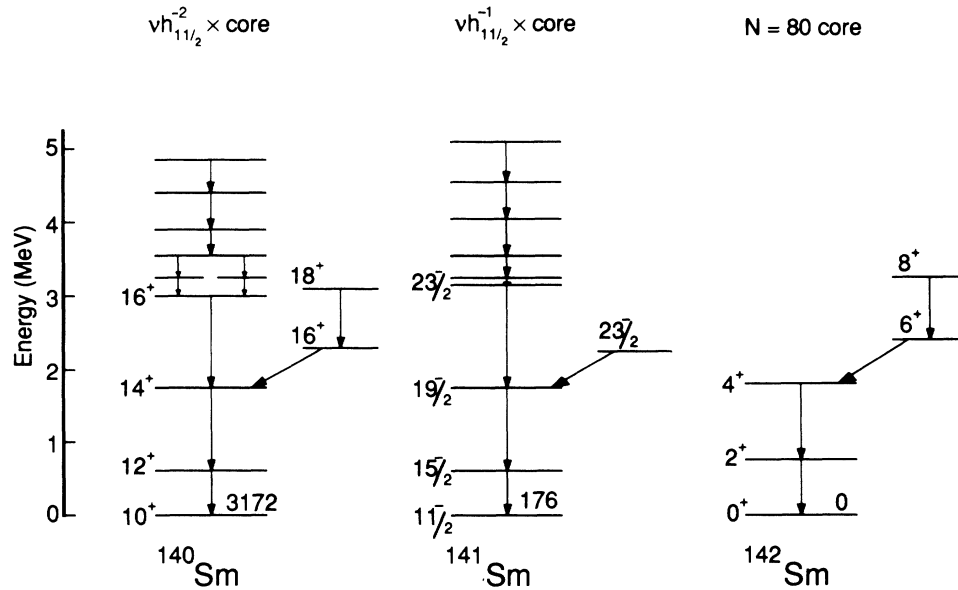


FIG. 3. The level spectrum built on the aligned $(\nu h_{11/2})^{-2} 10^+$ excitation in ^{140}Sm compared with some energy levels of the ^{141}Sm nucleus above the $h_{11/2}$ neutron state and with a partial level scheme of the core nucleus ^{142}Sm .

and the ^{139}Pm level scheme we are tempted to interpret in the same way the strong $\Delta I=1$ sequence built on the $I=16$ state at 5706 keV for which we suggest, therefore, a positive parity. Indeed shell model calculations with a surface delta residual interaction indicate that, while the maximum spin 20^+ of the $\pi h_{11/2}^2 \nu h_{11/2}^{-2}$ configuration is pushed up in energy, the $I_{\text{max}}-4(16^+)$ coupling is particularly lowered when compared with the other couplings of the same configuration. The same result is obtained for the $I_{\text{max}}-2$ coupling giving $I^\pi = \frac{27}{2}^-$ of the $\pi h_{11/2} \nu h_{11/2}^{-2}$ configuration in the odd nuclei ^{141}Eu and ^{139}Pm . The $\Delta I=1$ level sequence built on the $I=16$ level at 5706 keV may have the same structure of the sequence observed in the odd- Z nuclei above the $\frac{27}{2}^-$ state and which is interpreted as a band based on the $(\pi h_{11/2} \nu h_{11/2}^{-2})$ configuration with an oblate collective shape.²⁰

As we have compared the states of ^{140}Sm above the $(\pi h_{11/2})^2 10^+$ isomer with the one-proton nucleus ^{139}Pm , we will compare now the states built on the $(\nu h_{11/2})^{-2} 10^+$ isomer at 3172 keV with the $N=79$ nucleus ^{141}Sm , which has one neutron hole with respect to the core nucleus ^{142}Sm . In Fig. 3 the main gamma-ray cascade built on the 10^+ state of neutron character in ^{140}Sm is shown together with the excited states of ^{141}Sm above the $\frac{11}{2}^-$ state.¹⁹ In the same figure some of the excited states of the core ^{142}Sm are also reported.² The close similarity between this part of the ^{140}Sm excitation spectrum and the ^{141}Sm level scheme once more stresses the fact that the same core states are involved in the excited levels of both nuclei: in one case they are coupled to one $h_{11/2}$ neutron

hole, in the other case to two $h_{11/2}$ neutron holes.

Above 3.2 MeV there are two other series of excited states in the ^{140}Sm spectrum which we have not yet discussed and which are not easily understood in the framework we have used up to now. One of these series can be viewed as a band starting from the $I=15$ level at 4627 keV which deexcitates to the 14^+ level of the main cascade through a 218 keV transition. The excitation energy of the levels follow closely the $I(I+1)$ rule giving a possible indication of a rotational behavior. The other sequence of states is the only one observed in our experiment to deexcitate to both the $\pi h_{11/2}^2$ and $\nu h_{11/2}^{-2}$ aligned bands known to have opposite shapes. This level sequence connects therefore levels of opposite deformation, but, at the moment, the interpretation of such states is not clear.

V. CONCLUSIONS

The level scheme of ^{140}Sm has been extended up to $I=(22)$ and $E_x=8101$ keV. The rich level structure which is observed above the isomeric 10^+ states can be almost completely understood if one considers separately the states above the $(\pi h_{11/2})^2 10^+$ level and the states built on the $(\nu h_{11/2})^{-2} 10^+$ level. In both cases the excitation spectrum above the aligned 10^+ isomeric states is explained in terms of the coupling of two valence proton particles or neutron holes to the respective $N=78$ or 80 core nucleus. A remarkable agreement is observed between the level spectrum of the odd-even nuclei ^{139}Pm and ^{141}Sm (with respectively one particle and one hole outside the $N=78$ and 80 cores) and the excited states of ^{140}Sm .

*Also at Instituto de Fisica Corpuscolar, Valencia, Spain.

- ¹W. Starzecki, G. de Angelis, B. Rubio, J. Styczen, K. Zuber, H. Güven, W. Urban, W. Gast, P. Kleinheinz, S. Lunardi, F. Soramel, A. Facco, C. Signorini, M. Morando, W. Meczynski, A. M. Stefanini, and G. Fortuna, *Phys. Lett. B* **200**, 419 (1988).
- ²M. Lach, J. Styczen, R. Julin, M. Piiparinen, H. Beuscher, P. Kleinheinz, and J. Blomqvist, *Z. Phys. A* **319**, 235 (1984).
- ³T. Morek, H. Beuscher, B. Bochev, D. R. Haenni, R. M. Lieder, T. Kutzarova, M. Müller-Veggian, and A. Neskakis, *Z. Phys. A* **298**, 267 (1980).
- ⁴D. Bazzacco, F. Brandolini, K. Loewenich, S. Lunardi, P. Pavan, C. Rossi-Alvarez, F. Soramel, M. De Poli, A. M. I. Haque, and G. de Angelis, *Phys. Lett. B* **206**, 404 (1988).
- ⁵D. Bazzacco, F. Brandolini, K. Loewenich, P. Pavan, C. Rossi-Alvarez, M. De Poli, and A. M. I. Haque, Report No. LNL-INFN (REP)-014/88, 1988, p. 7.
- ⁶J. Meyer-Ter-Vehn, *Nucl. Phys. A* **249**, 111 (1975), **A249**, 141 (1975).
- ⁷G. Alaga and V. Paar, *Phys. Lett.* **61B**, 129 (1976).
- ⁸M. Müller-Veggian, Y. Gono, R. M. Lieder, A. Neskakis, and C. Mayer-Böricke, *Nucl. Phys. A* **304**, 1 (1978).
- ⁹J. Gizon, A. Gizon, R. M. Diamond, and F. S. Stephens, *J. Phys.* **64**, L171 (1978).
- ¹⁰M. Piiparinen, M. Kortelahti, A. Pakkanen, T. Komppa, and R. Komu, *Nucl. Phys. A* **342**, 57 (1980).
- ¹¹G. Lo Bianco, N. Molho, P. Sala, D. Bazzacco, A. Buscemi, S. Lunardi, M. Morando, G. Nardelli, F. Soramel, A. M. Bizzeti Sona, P. G. Bizzeti, A. Brondi, and F. Terrasi, Report No. LNL-INFN (REP)-014/88, 1988, p. 129.
- ¹²M. Müller-Veggian, H. Beuscher, D. R. Haenni, R. M. Lieder, A. Neskakis, and C. Mayer-Böricke, *Nucl. Phys. A* **344**, 89 (1980).
- ¹³E. Dafni, J. Bendahan, C. Braude, G. Goldring, M. Hass, E. Naim, M. H. Rafailovich, C. Chasman, O. C. Kistner, and S. Vojda, *Phys. Rev. Lett.* **53**, 2473 (1984).
- ¹⁴E. Dafni, J. Bendahan, C. Braude, G. Goldring, M. Hass, E. Naim, and M. H. Rafailovich, *Phys. Lett. B* **181**, 21 (1986).
- ¹⁵N. Xu, C. W. Beausang, E. S. Paul, W. F. Piel, P. K. Weng, D. B. Fossan, E. Gülmez, and J. A. Cizewski, *Phys. Rev. C* **36**, 1649 (1987).
- ¹⁶H. Güven, R. Julin, M. Lach, J. Styczen, M. Müller-Veggian, A. Krämer-Flecken, and P. Kleinheinz, *Z. Phys. A* **330**, 437 (1988).
- ¹⁷D. Bazzacco, S. Lunardi, and G. Nardelli (unpublished).
- ¹⁸D. Bazzacco, S. Lunardi, J. Rico, F. Soramel, A. M. Bizzeti-Sona, P. G. Bizzeti, F. Banci-Buonamici, N. Blasi, R. Garavaglia, G. Lo Bianco, N. Molho, A. J. Kirwan, J. Simpson, G. de Angelis, P. Kleinheinz, and W. Starzecki, in *Proceedings of the Third International Conference on Nucleus-Nucleus Collisions, Saint-Malo, France, 1988*, edited by C. Esteve, C. Gregoire, D. Guerra and B. Tamain (Centre de Publication de l'Université de Caen, Caen, 1988), p. 31.
- ¹⁹D. Bazzacco, M. De Poli, and S. Lunardi (unpublished).
- ²⁰N. Xu, C. W. Beausang, R. Ma, E. S. Paul, W. F. Piel, and D. B. Fossan, *Phys. Rev. C* **39**, 1799 (1989).